Plasticization of Polylactide with Block Copolymers of Ethylene Glycol and Propylene Glycol

Marcin Kowalczyk,[1] Miroslaw Pluta,[1] Ewa Piorkowska,[1] Nelli Krasnikova[1,2]

[1]*Centre of Molecular and Macromolecular Studies, Polish Academy of Sciences, Sienkiewicza 112, 90-363 Lodz, Poland*
[2]*Topchiev Institute of Petrochemical Synthesis, Russian Academy of Sciences, Leninsky Prospekt 29, 117912 Moscow, Russia*

Received 30 November 2011; accepted 30 November 2011
DOI 10.1002/app.36563
Published online in Wiley Online Library (wileyonlinelibrary.com).

ABSTRACT: In this study, plasticization of polylactide (PLA) with PEG–PPG–PEG triblock copolymers was examined. Two different copolymers were utilized, with molecular weight of 1100 and 1900 g mol^{-1}, and with PEG contents of 10 and 50 wt %, respectively. A PPG plasticizer with molecular weight of 1000 g mol^{-1}, close to that of PPG block in the copolymers, was also used for comparison. Melt blends containing 10 and 15 wt % of the plasticizers were prepared. Thermal properties, mechanical properties, and structure of quenched and annealed films of the blends were studied. The crystallization driven phase separation occurred in all the annealed blends but led to different structures depending on the plasticizer used. Distinct inclusions of the plasticizer were visible under the scanning electron microscope only in PLA with PPG but not in the blends of PLA with the copolymers. The drawability of the plasticized systems was improved when compared with neat PLA. In the quenched and annealed blends, elongations at break at the level of 5 and 0.7, respectively, were reached. © 2012 Wiley Periodicals, Inc. J Appl Polym Sci 000: 000–000, 2012

Key words: polylactide; plasticization; cold crystallization; mechanical properties

INTRODUCTION

Polylactide (PLA), a biodegradable and biocompatible aliphatic polyester, can also be produced from annually renewable resources such as sugar beets, corn starch, rice, and wheat.[1,2] This fact is responsible for a growing interest in PLA applications, for instance, in the field of rigid packaging, flexible film packaging, injection molded products, and textile fiber production.[3] Owing to relatively high glass transition temperature, T_g, in the range of 55–60°C, PLA is stiff and brittle at room conditions, which limits its applications demanding high toughness and drawability.

Chiral center in the structure allows us to vary the enantiomeric compositions of PLA. Both optically pure poly(L-lactide) and poly(D-lactide) are crystallizable polymers, but monomers of different chirality in the PLA chain decrease its ability to crystallize. Slowly crystallizing PLAs could be quenched below T_g and cold crystallized during subsequent heating from the glassy state.[4] Crystallinity, if developed, increases slightly the modulus of elasticity and further decreases the drawability of PLA.[5]

Recently, a significant engineering effort was made to improve PLA's mechanical properties. To modify the mechanical properties PLA was plasticized with various substances differing in chemical structure and molecular weight, for example lactide monomer,[1] poly(3-methyl-1,4-dioxan-2-one),[6] poly (ethylene oxide),[7] citrate esters,[8,9] triacetine,[9] poly (ethylene glycol) (PEG),[10–15] and poly(propylene glycol) (PPG).[16,17] A very important aspect of plasticization is stability of a plasticized polymer. For example, PEG with M_n of 1000 g mol^{-1} diffuses from the PLA bulk toward the surface.[18] Moreover, the phase separation and crystallization of PLA and/or PEG can occur in a degree dependent on optical purity of PLA, concentration, and molecular weight of PEG.[14,18,19] The phase separation and crystallization of PEG increases the stiffness and deteriorates the drawability of plasticized PLA.

It has to be emphasized that a significant decrease of T_g due to plasticization excludes the use of amorphous PLA at elevated temperature. However, crystallization increases the upper temperature limit of applicability up to the melting temperature of crystals, usually much higher than T_g of the amorphous

Correspondence to: E. Piorkowska (epiorkow@cbmm.lodz.pl).

Contract grant sponsor: European Union European Regional Development Fund; contract grant number: POIG.01.03.01-00-018/08-00.

Contract grant sponsors: Polish Academy of Sciences (PAS) and the Russian Academy of Sciences (RAS).

phase. Thus, effective plasticization of the amorphous phase of semicrystalline PLA would lead to a material with a greatly broadened range of potential applications. Moreover, crystallinity improves barrier properties of PLA.[20]

Crystallization in the plasticized PLA not only increases a plasticizer content in the amorphous phase but, in addition, can lead to excessive accumulation of a plasticizer in front of growing spherulites and, finally, in interspherulitic boundaries which can result in premature fracture during drawing.[15,17]

Recently,[21,22] plasticization of PLA, both amorphous and semicrystalline, with 5–20 wt % of random copolymer of ethylene glycol and propylene glycol (PEPG), with M_n of 12 kg mol^{-1} and ethylene glycol content about 80 mol %, was reported. Crystallization in the plasticized PLA of low optical purity resulted in brittle materials, whereas crystallized plasticized PLA of higher optical purity could be drawn to elongations of about 65%. In our previous works, we found that PPG with nominal M_n of 425 or 1000 g mol^{-1} efficiently plasticized amorphous PLA, and it was also a good plasticizer for semicrystalline PLA, better than PEG with similar molecular weight.[16,17] Moreover, in contrast to PEG, PPG has no ability to crystallize and, if phase separated from PLA, it remained in the liquid state and did not deteriorate the drawability of the blend.

Disadvantageous phenomena related to diffusion of the plasticizer can be limited by an increase of the plasticizer's molecular weight. The increase of molecular weight can hinder migration of the plasticizer to the surface and also diffusion during crystallization in the plasticized PLA. On the other hand, it can worsen the efficiency of plasticization increasing T_g of a blend[13] and, as a consequence, higher plasticizer content is required to reach desired properties. Moreover, higher molecular weight of the plasticizer can worsen the miscibility and facilitate phase separation in the blend, for instance a solubility limit of PEG with molecular weight increasing from 400 to 10,000 g mol^{-1} decreases from 30 to 15 wt %.[13] Solubility of PPG in PLA is worse, for instance in Ref. [16] traces of phase separation were found in PLA plasticized with 12.5 wt % of PPG having M_n of 1000 g mol^{-1}. It can be expected that marked increase of molecular weight of PPG above 1000 g mol^{-1} will further decrease the solubility limit.

To increase molecular weight of a plasticizer and taking advantage of better miscibility of PEG with PLA, we used triblock copolymers of propylene glycol and ethylene glycol having the structure PEG–b-PPG–b-PEG, with the central PPG block of molecular weight about 1000 g mol^{-1}, flanked by PEG blocks of different length. We compared the plasticization of PLA with the copolymers and with PPG having nominal M_n of 1000 g mol^{-1}. Our study provided therefore information about the role of end PEG blocks in the plasticization of PLA, as well as structure and properties of plasticized PLA, both amorphous and cold crystallized.

EXPERIMENTAL

Materials

Polylactide PLA 2002D, with density of 1.24 g cm^{-3} and melt flow index of 5–7 g/10 min (210°C, 2.16 kg) was produced by NatureWorks LLC (Minnetonka, MN). M_w of 104 kg mol^{-1} and M_w M_n^{-1} =1.4 were determined by size-exclusion chromatography (SEC) with multi-angle laser light scattering (MALLS) detector in dichloromethane. The D-lactide and L-lactide contents were 2.5% and 97.5% as calculated based on specific optical rotation measurements.

PPG with nominal M_n of 1000 g mol^{-1} and two triblock copolymers, PEG–b-PPG–b-PEG, Pluronic L31, and Pluronic L35 were purchased from Sigma Aldrich (St. Louis, MO). According to the supplier, M_n and PEG content were 1100 g mol^{-1} and 10 wt % for Pluronic L31 (EPE11), whereas 1900 g mol^{-1} and 50 wt % for Pluronic L35 (EPE19). In the molecule of EPE11, the central PPG block of 990 g mol^{-1} is flanked by two PEG blocks with total molecular weight of 110 g mol^{-1}, whereas corresponding numbers for EPE19 are 950 and 950 g mol^{-1}. It appears that the copolymers are built of the central PPG blocks of nearly the same length as the molecule of PPG homopolymer and, in addition, end PEG blocks of different lengths.

Molecular characteristics of the plasticizers were verified by a matrix-assisted laser desorption/ionization time-of-flight (MALDI TOF) technique, in a linear mode, using a Voyager-Elite instrument (PerSeptive Biosystems, Framingham, MA) equipped with a pulsed N2 laser. The matrix, 2,5-dihydroxybenzoic acid, and the cationizing agent, NaI, were dissolved in water. M_n and M_w/M_n determined from the spectra using the Data Explorer program were 1073 g mol^{-1} and 1.02 for PPG, 1180 g mol^{-1} and 1.05 for EPE11, and 1940 g mol^{-1} and 1.04 for EPE19.

Differential scanning calorimetry (DSC) heating thermograms of the plasticizers recorded at the heating rate of 10°C min^{-1} using a Diamond DSC Perkin Elmer instrument (Waltham, MA) are compared in Figure 1. T_gs of PPG, EPE11 and EPE19 were at −70, −71, and −70°C, respectively. During cooling at 10°C min^{-1}, EPE19 crystallized with a peak at −16°C. During subsequent heating, it exhibited melting with a peak at 10°C. The melting enthalpy of 52 J g^{-1} corresponds to crystallinity level of PEG blocks of 35 wt % (assuming the enthalpy of fusion of 146.7 J g^{-1} for 100% crystalline PEG[24]).

Sample preparation

Before blending, the polymers were vacuum dried at 100°C for 4 h. Melt blends containing 10 and 15 wt % of plasticizers were prepared using a Brabender

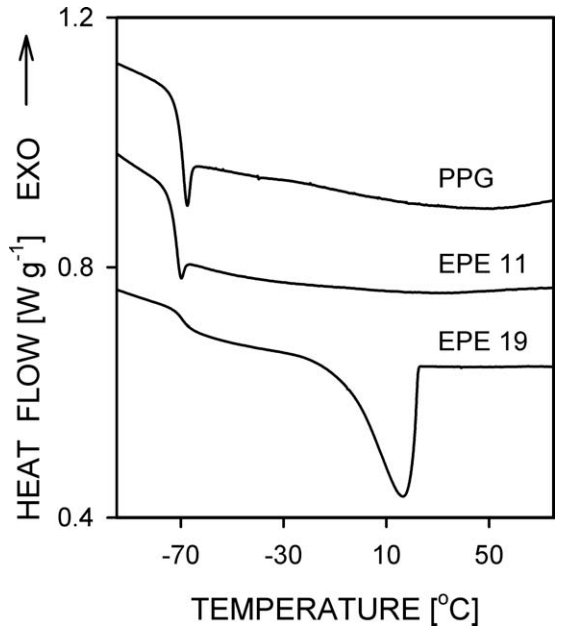

Figure 1 DSC heating thermograms of plasticizers: PPG, EPE11 and EPE19. Heating rate 10°C min^{-1}. Thermograms shifted for clarity.

mixer (Duisburg, Germany) operating at 190°C for 15 min at 60 rpm, under the flow of dry gaseous nitrogen. Neat PLA was also processed in the same way to obtain a reference material. The blends with PPG, EPE11, and EPE19 will be referred to through the paper as PLA/P10, PLA/EPE11, and PLA/EPE19, respectively, with a number indicating percentage of plasticizer, for instance, PLA/P10-10 for the blend of PLA with 10 wt % of PPG.

A 0.5 mm and 1 mm thick films of PLA and plasticized PLA were prepared by compression molding at 180°C for 3 min in a hydraulic hot press followed by quenching between thick metal blocks kept at room temperature. To have crystalline materials, some of the films were annealed between two metal blocks, equipped with heaters and Pt resistance thermometers connected to a temperature controller. The films were heated at the rate of about 8–10°C min^{-1} from room temperature to 120°C, kept at this temperature for 2–3 min, and quenched to room temperature. Other details of the method are given elsewhere.[15] Cold crystallization was chosen as a crystallization method because it led to a more intense spherulite nucleation resulting in a shorter crystallization time and smaller spherulites.[4] Precrystallization thermal treatment and crystallization conditions were selected based on preliminary studies of all materials involving DSC, carried out with a TA Instrument 2920 DSC (New Castle, DE) on 10–12 mg specimens.

Sample examination

The films, both quenched and annealed, were characterized by the DSC technique with a TA Instrument 2920 DSC during heating from 0 to 200°C at the heating rate of 10°C min^{-1} under a flow of dry gaseous nitrogen. Selected samples were examined during heating from −50°C. T_g of all the materials was measured as the temperature corresponding to the midpoint of the heat capacity increment.

Dynamic mechanical properties of the materials were tested on rectangular specimens, 28 mm × 10 mm, cut out from 1 mm films, in the dual cantilever mode in a dynamic mechanical thermal analysis (DMTA) Mk III, Rheometric Scientific Ltd. apparatus (Epsom, UK) at the frequency of 1 Hz, during heating from −100 to 100°C at the rate of 2°C min^{-1}.

To have an insight into blend morphology, 0.5 mm thick films of all materials were submerged in liquid nitrogen and broken; the cryofracture surfaces of these films were examined under the scanning electron microscope (SEM), Jeol 5500LV (Tokyo, Japan), after sputtering with gold.

Tensile tests were performed on an Instron machine (High Wycomb, UK) at 20°C, at the rate of 0.5 min^{-1}, on oar-shaped specimens, conforming to ISO-527 type 1A with 20 mm gauge length and gauge width of 5 mm cut out from 0.5 mm thick films.

The gauge regions of deformed specimens of the quenched blends with 15 wt % of plasticizers were examined by 2D wide angle X-ray scattering (WAXS) by using WAXS camera coupled to the X-ray generator (sealed-tube, fine point CuK_α filtered source operating at 30 kV and 50 mA, Philips, Eindhoven, The Netherlands) and imaging plates for recording the diffraction patterns. The undeformed specimens were also studied for comparison.

RESULTS AND DISCUSSION

Heating thermograms of the quenched films are collected in Figure 2. Above glass transition, the samples cold crystallized and melted when the temperature increased. T_g of neat PLA was about 60°C, whereas the cold crystallization exhibited maximum rate at T_c of 127°C. In the materials with 10 and 15 wt % of the plasticizers, T_g decreased to 39–40°C and to 32–35°C, respectively. It can also be noticed that the glass transition broadened with an increase of the plasticizer content. Plasticization resulted in narrowing of cold crystallization peaks and a decrease of T_c to the range of 82–99°C, although long tails followed the crystallization peaks of the blends until melting. PLA/P10-10 was exceptional, with a relatively broad crystallization exotherm with T_c of 115°C.

Melting of the neat PLA and PLA/P10-10 started before the completion of crystallization. The thermogram of PLA exhibited a single melting peak centered at about 152°C, whereas that of PLA/P10-10 was featured by a melting endotherm with two

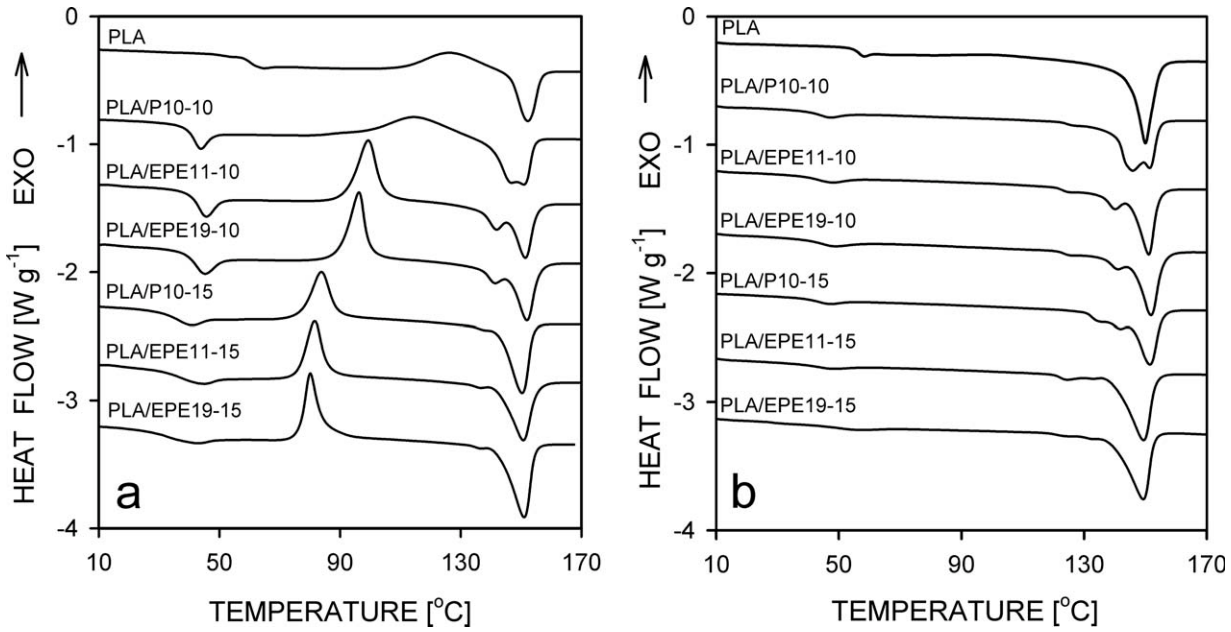

Figure 2 DSC heating thermograms of PLA and PLA blends with plasticizers: (a) quenched films and (b) annealed films. Heating rate 10°C min^{-1}. Thermograms shifted for clarity.

peaks, at 147 and at 151°C. In the case of other quenched materials, the main melting peaks at 150–152°C were preceded by smaller ones centered at lower temperatures, decreasing with plasticizer contents. For the blends with 15 wt % of plasticizers these peaks became hardly visible.

The cold crystallization enthalpy, ΔH_c, of quenched PLA, 16 J g^{-1}, was equal to the melting enthalpy, ΔH_m, evidencing that the sample was amorphous before heating in the DSC. The same applies to PLA/P10-10 and PLA/P10-15 with ΔH_c of 26 and 30 J $(g_{PLA})^{-1}$, respectively, and to the blends with copolymers with ΔH_c equal to 29 J $(g_{PLA})^{-1}$.

Heating thermograms of the annealed films are shown in Figure 2(b). Above glass transition, only melting of PLA crystals occurred which evidenced that crystallization in these materials was accomplished during annealing. It can be noticed that the glass transition in the annealed films is less pronounced than on the thermograms of corresponding quenched films. This resulted not only from a decreased amount of the amorphous phase but also from broadening of the transition. T_g of neat PLA was about 60°C, whereas in the blends with 10 wt % of plasticizers it decreased to about 40–41°C. In the blends with 15 wt % of plasticizers glass transition became so broad that nearly indistinguishable. The melting of all materials started above 100°C. The melting peaks, similar to those visible on the thermograms of the quenched blends in Figure 2(a), were preceded by very small peaks which were most probably connected with a minute fraction of thinner and/or less perfect crystals formed during quenching of the films to room temperature after annealing. The ΔH_m of neat PLA was 34 J g^{-1}, whereas that of the plasticized PLA varied in the range of 33–37.5 J $(g_{PLA})^{-1}$, which corresponded to the crystallinity level of 31–35 wt % if the enthalpy of fusion of 106 J g^{-1} was assumed.[25]

No evidence of melting of EPE19 was found on heating thermograms of PLA/EPE19-15, either quenched or annealed, although the blends were cooled to −50°C before heating to make crystallization of EPE19 possible.

Temperature dependencies of the loss modulus, E'', for the materials studied are plotted in Figure 3(a,b), whereas temperatures of E'' and tan δ peaks denoted as $T_{E''}$ and $T_{\tan\,\delta}$, respectively, are listed in Table I. Quenched PLA exhibited a single E'' peak at 57°C. In general, plasticization caused a decrease of $T_{E''}$ and also broadening of the peak. Quenched PLA/P10-10 and PLA/EPE11-10 exhibited single E'' peaks, at $T_{E''}$ shifted to 41°C due to plasticization. A trace of E'' peak at −57°C, in addition to the main E'' peak at 39°C, became visible for PLA/EPE19-10. An increase of PPG content to 15 wt % reduced $T_{E''}$ to 36°C. Moreover, a broad shoulder, extending to about −70°C, appeared on the low temperature slope of the peak. Quenched PLA/EPE11-15 and especially PLA/EPE19-15 exhibited single broad peaks, with $T_{E''}$ of 35 and 28°C, respectively, with pronounced low temperature shoulders.

Each quenched material exhibited single tan δ peak with $T_{\tan\delta}$ exceeding $T_{E''}$. Plasticization resulted in the broadening of peaks and decrease of $T_{\tan\delta}$ enhanced by the higher plasticizer content.

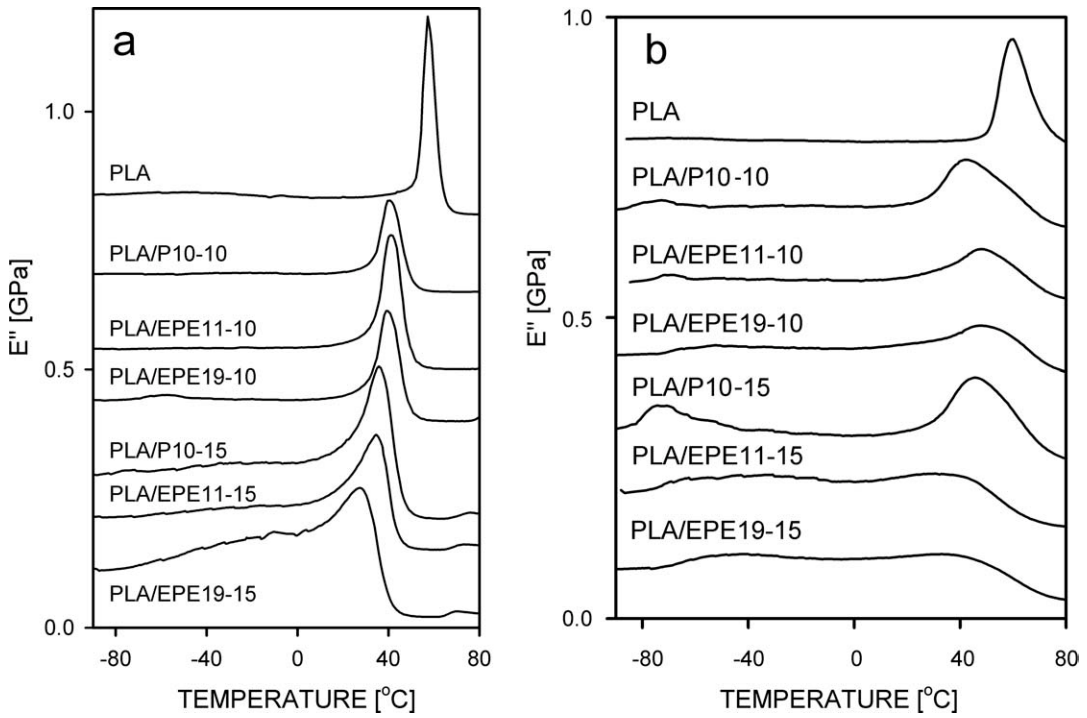

Figure 3 Temperature dependencies of loss modulus E'': (a) quenched films and (b) annealed films. Heating rate 2°C min^{-1}, frequency 1 Hz. Plots shifted for clarity.

Moreover, the difference between $T_{tan\delta}$ and $T_{E''}$ increased with an increasing plasticizer content providing further evidence of the broadening of glass transition.

Among the annealed materials only neat PLA exhibited a single peak of E'' at 60°C, whereas for all annealed blends two peaks were recorded, corresponding to glass transitions in PLA rich phase and plasticizer rich phase, evidencing the crystallization driven phase separation. For PLA/P10-10 and PLA/P10-15 $T_{E''}$ of the PLA rich phase was equal to 42 and 46°C, respectively, whereas that of the PPG rich phase was equal to −72 and −71°C, respectively; the low temperature peak was more pronounced for PLA/P10-15. Plasticization of PLA with 10 and 15 wt % of EPE11 and EPE19 resulted in shifting of high temperature E'' peaks to 48°C and to 30–33°C, respectively. A small low temperature E'' peak appeared at −69°C in the case of PLA/EPE11-10. Low temperature E'' peaks of the other three blends were very broad with $T_{E''}$ ranging from −52 to −40°C. Broadness of the E'' peaks is suggestive of concentration gradients in both PLA and plasticizer rich phases.

TABLE I
Temperatures of Loss Modulus Peaks, $T_{E''}$, and tan δ Peaks, $T_{tan\ \delta}$, of Quenched and Annealed PLA and PLA Blends with Plasticizers

Sample code	Quenched		Annealed	
	$T_{E''}$ (°C)	$T_{tan\ \delta}$ (°C)	$T_{E''}$ (°C)	$T_{tan\ \delta}$ (°C)
PLA 2002D	−, 57	64	−, 60	−, 66
PLA/P10–10	−, 41	50	−72, 42	−71, 62
PLA/EPE11–10	−, 41	50	−69, 48	−68, 65
PLA/EPE19–10	−57, 39	49	−52, 48	−, 65*
PLA/P10–15	−, 36*	48	−71, 46	−70, 66
PLA/EPE11–15	−, 35*	46	−43, 30	−, 54*
PLA/EPE19–15	−, 28*	43	−40, 33	−, 62*

The minus sign denotes the absence of a low temperature peak and the asterisk denotes a peak with low temperature shoulder.

$T_{tan\delta}$ of each annealed material, 66°C for neat PLA and 54–66°C for plasticized PLA, exceeded $T_{E''}$. $T_{tan\delta}$ of PLA plasticized with copolymers decreased with increasing plasticizer contents. Contrary to this, an increase of the PPG content resulted in elevation of $T_{tan\delta}$. It can be noticed that the annealing of blends broadened the tan δ peaks and increased the difference between $T_{tan\delta}$ and $T_{E''}$ to 20–24°C. It is observed that the crystallization driven phase separation resulted in the appearance of either low temperature shoulders of tan δ peaks or additional small peaks at low temperatures.

Examples of SEM micrographs of the materials studied are shown in Figures 4 and 5. In quenched PLA/P10-15 submicron holes, where PPG was accumulated, were occasionally seen, as shown in Figure 4(b). Numerous larger holes, with sizes reaching up to two micrometers, were observed on cryofracture surfaces of annealed PLA/P10-10 and PLA/P10-15, as illustrated in Figure 5(b,c). On cryofracture surface of the latter also submicron holes were found, visible in the inset in Figure 5(c). No heterogeneities

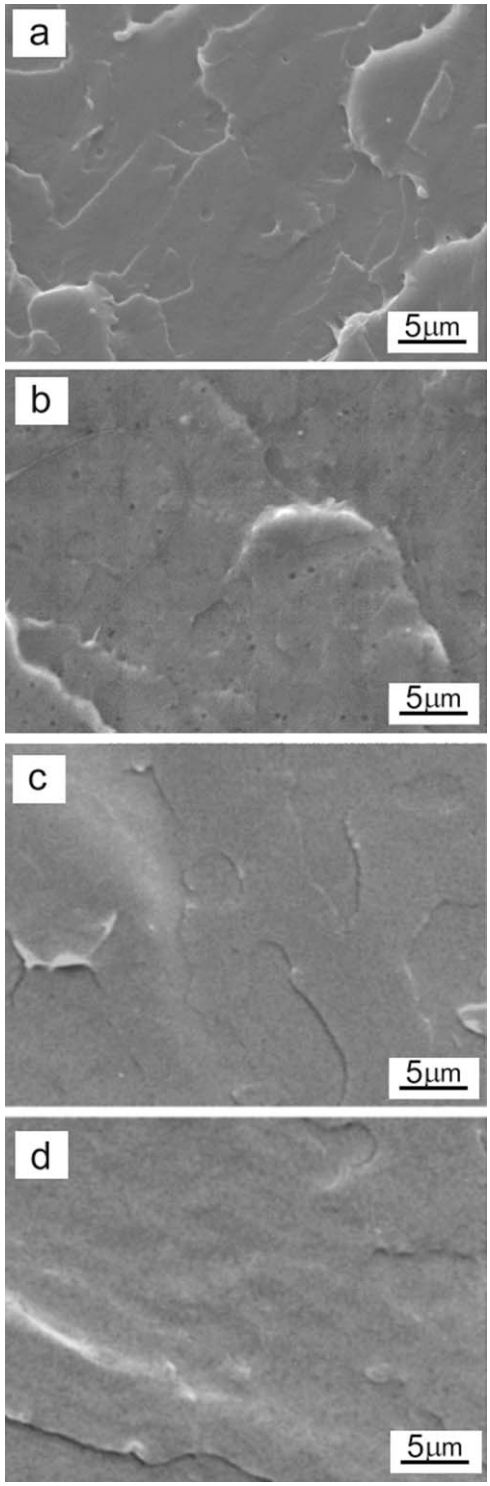

Figure 4 SEM micrographs of cryofracture surfaces of quenched films: (a) PLA, (b) PLA/P10-15, (c) PLA/EPE11-15, and (d) PLA/EPE19-15.

suggestive of phase separation were observed by the SEM technique in the other systems studied, including annealed PLA/EPE11-15 (not shown) and PLA/EPE19-15 shown in Figure 5(d).

The stress–strain dependencies of the materials studied are collected in Figure 6(a,b), whereas the average values of mechanical parameters measured during tensile experiments are compared in Table II. Quenched neat PLA yielded at 61 MPa and fractured at the strain and stress of 0.06 and 59 MPa, respectively. Quenched samples with 10 wt % of plasticizers exhibited the decreased yield stress, 51–56 MPa, and stress at break, 38–52 MPa, whereas the average elongation at break of these materials remained nearly the same as that of neat PLA. An increase of PPG content to 15 wt % lowered the

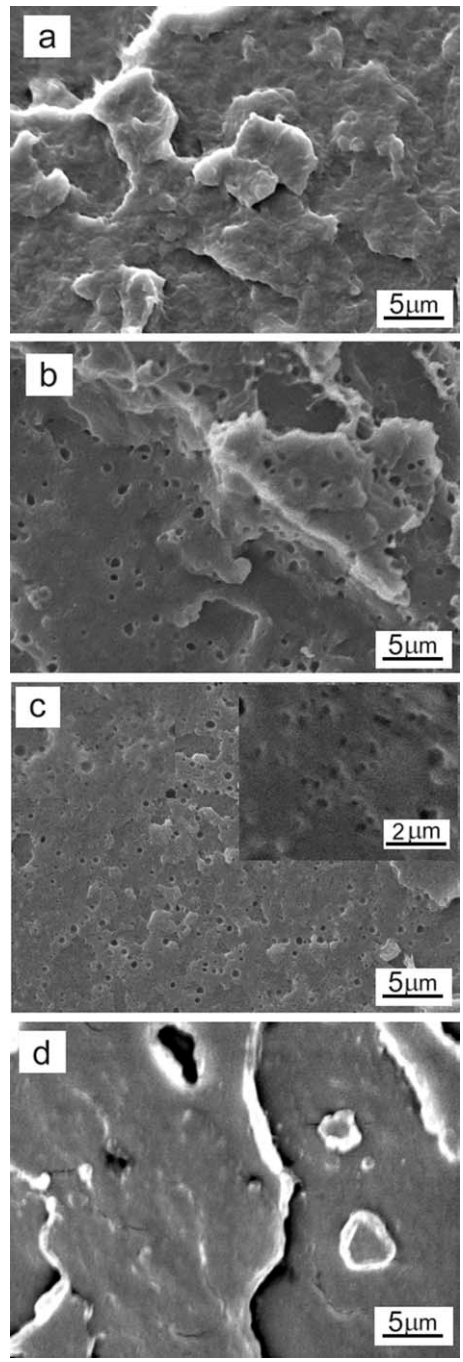

Figure 5 SEM micrographs of cryofracture surfaces of annealed films: (a) PLA, (b) PLA/P10-10, (c) PLA/P10-15, and (d) PLA/EPE19-15.

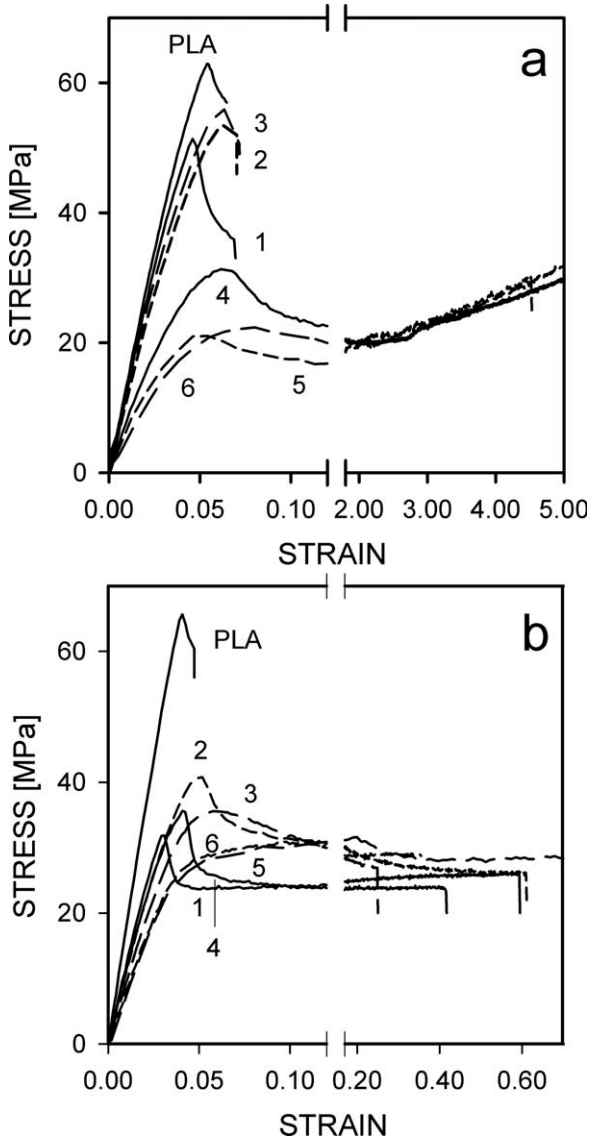

Figure 6 Stress–strain dependencies of PLA and PLA blends with plasticizers: (a) quenched and (b) annealed. 1-PLA/P10-10, 2-PLA/EPE11-10, 3-PLA/EPE19-10, 4-PLA/P10-15, 5-PLA/EPE11-15, and PLA/EPE19-15.

TABLE II
Mechanical Properties (Average Values) of Quenched and Annealed PLA and PLA Blends with Plasticizers: σ_y – Yield Stress, σ_b – Stress at Break, and ε_b – Elongation at Break

	Quenched			Annealed		
Sample code	σ_y (MPa)	σ_b (MPa)	ε_b	σ_y (MPa)	σ_b (MPa)	ε_b
PLA	61	59	0.06	65	60	0.05
PLA/P10–10	51	38	0.07	32	26	0.71
PLA/EPE11–10	54	52	0.07	42	29	0.36
PLA/EPE19–10	56	51	0.07	35	26	0.21
PLA/P10–15	32	30	5.10	35	23	0.32
PLA/EPE11–15	21	30	4.60	30	25	0.59
PLA/EPE19–15	22	32	5.10	30	28	0.72

yield stress to about 32 MPa. A stronger decrease of the yield stress, to 21–22 MPa, was observed in the case of PLA plasticized with 15 wt % of the copolymers. Regardless of the plasticizer used, the elongation at break of the quenched blends with 15 wt % of plasticizers was dramatically improved in comparison to neat PLA and reached nearly 5. At strains larger than 2, all three materials behaved similarly showing strong strain-hardening, which resulted in the stress at break ranging from 30 to 32 MPa.

Figure 7 shows a comparison of exemplary 2D-WAXS patterns recorded for the specimens of quenched PLA/P10-15, PLA/EPE11-15, and PLA/EPE19-15. The diffuse amorphous halo without any reflections from the crystalline phase, visible on patterns shown in Figure 7(a,c,e), evidences that the quenched blends were amorphous before tensile experiments. The 2D-WAXS pattern of each deformed blend displays a very strong polar reinforcement of the halo, which according to Ref. [26] provides evidence of the mesomorphic phase of PLA. According to Ref. [26], the mesomorphic phase forms during uniaxial drawing of neat PLA below

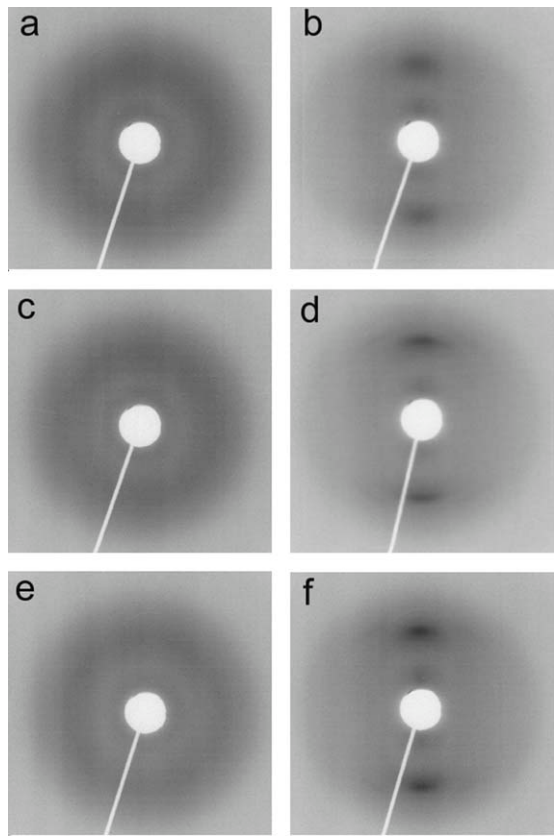

Figure 7 2D-WAXS patterns of quenched films of PLA blends with plasticizers: (a) PLA/P10-15 before deformation, (b) PLA/P10-15 deformed to strain of 5.9, (c) PLA/EPE11-15 before deformation, (d) PLA/EPE11-15 deformed to strain of 5.9, (e) PLA/EPE19-15 before deformation, and (f) PLA/EPE19-15 deformed to strain of 5.1. Drawing direction—horizontal.

75°C and the onset of growth of the mesomorphic phase appears close to the onset of strain-hardening. It has to be emphasized that the strain-induced crystallization during uniaxial drawing of PLA plasticized with either PEG or PPG was already evidenced in Refs. 15, 16, but the formation of the mesomorphic phase in these systems was not reported.

Annealing increased slightly the yield stress of PLA to 65 MPa, whereas the stress and elongation at break remained practically the same. Annealing of PLA/P10-10 significantly decreased the tensile stresses, at yield to 32 MPa, and at break to 26 MPa, and also markedly improved elongation at break to about 0.7. An increase of PPG content to 15 wt % resulted in a slight elevation of the yield stress but reduced the strain at break to 0.3. PLA/EPE11-10 and PLA/EPE19-10 exhibited the yield stresses of 42 and 35 MPa, respectively, and elongations at break of about 0.4 and 0.2, respectively. It can be noticed that the increase of copolymer content to 15 wt % resulted in a decrease of the yield stress to 30 MPa and increase of the elongation at break, to 0.6–0.7. Annealed PLA/EPE11-15 and PLA/EPE19-15 behaved in a similar way, with plastic deformation beginning below 30 MPa and without a pronounced yield. The stress at break of all annealed blends with 15 wt % of plasticizers was in the range of 23–28 MPa.

The plasticization of the PLA with PPG and triblock copolymers, PEG–b-PPG–b-PEG, effectively lowered T_g. The quenched materials showed clearly a decrease of T_g due to enhanced segmental mobility of PLA chains caused by plasticization, increasing with plasticizer content. T_g of the quenched PLA blends with 10 wt % of plasticizers was similar; the blends were homogeneous with the exception of PLA/EPE19-10. An increase of the copolymer content to 15 wt % resulted not only in a further decrease of T_g but caused also broadening of the glass transition. Moreover, pronounced shoulders appearing on the E'' peaks, extending into low temperature region, especially for PLA/EPE19-15, indicated changes in the structure although no evidence of phase separation in the blends with copolymers was found by the SEM technique. The presence of few plasticizer inclusions in the PLA matrix was confirmed by SEM only in PLA/P10-15.

It can be concluded that, owing to the presence of PEG blocks, the phase separation in PLA blends with the copolymers has a different character than in PLA/P10 blends. SEM, DSC, and DMTA results suggest the presence of the copolymer enriched phase but not in the form of distinct inclusions dispersed in the PLA matrix.

It is known that the cold-crystallization temperature of PLA decreases in parallel with the shift in T_g caused by plasticization. T_c of PLA was more decreased in the blends with the copolymers than in the PLA/P10 blends, although the difference was much larger in the case of the materials with plasticizer content of 10 wt %. It was already reported that PPG influenced less the cold-crystallization behavior of PLA than PEG of similar molecular weight, despite the same effect on the glass transition.[16,17] A detailed explanation of differences in the crystallization of PLA in blends with polyglycols with different molecular structures requires, however, further studies.

Plasticization, decreasing T_c of the blends, affected also the melting process in these materials. The blends with 10 wt % of plasticizers exhibited double melting peaks. Others[7,27] already explained the additional melting peaks which appear on the DSC thermograms of plasticized and neat PLA as related to the reorganization of crystal structure. Further lowering of T_c caused by increased plasticizer content was accompanied by a reduction of those additional peaks; most possibly reorganization of the structure occurred during postcrystallization heating in the DSC.

Mechanical properties of the quenched blends were similar, regardless of the plasticizer used and differences in the structure. 10 wt % of plasticizer reduced the yield stress but did not improve elongation at break. A significant improvement of drawability required an increase of the plasticizer content to 15 wt % to ensure sufficient segmental mobility of the amorphous phase. It appears that the plasticizer content was a decisive factor governing the tensile behavior of blends.

DSC studies of the annealed blends evidenced that crystallization in these materials was accomplished during annealing. Glass transition of the PLA rich phase in the blends became nearly indistinguishable on the DSC thermograms due to a reduced amount of the amorphous phase but also due to a significant broadening of the transition. DMTA studies confirmed a decrease of T_g of the PLA rich phase due to the plasticization and also broadening of glass transition. Crystallization of PLA exuded plasticizers into the amorphous phase and increased their content in this phase by approx. 50% which caused the phase separation.

The phase separation in PLA/P10 blends was evidenced by low temperature E'' peaks at temperatures close to T_g of PPG and also by SEM examination. Owing to the crystallization-induced phase separation T_g of PLA/P10 blends increased after annealing. It can be noticed that $T_{E''}$ of the high temperature peak of PLA/P10-15 was higher than that of PLA/P10-10 despite the larger content of PPG. The phase separation was observed already in quenched PLA/P10-15, but it was strongly enhanced by crystallization, as confirmed by E'' plots. It can be noticed that T_c of quenched PLA/P10-15 was by approx. 30°C lower than that of quenched PLA/P10-10. During annealing, the quenched films were

heated at a similar rate and therefore crystallized in a similar temperature range as during heating in the DSC. Hence, it can be hypothesized that the phase separation in the annealed PLA/P10 blends was related to their different crystallization temperatures.

E'' plots demonstrate the phase separation also in the annealed PLA blends with copolymers. After crystallization in these blends, $T_{E''}$ of the PLA rich phase increased in all these materials except for PLA/EPE11-15, although in all cases $T_{E''}$s of high temperature E'' peaks of the blends with 15 wt % of copolymers remained lower than those of the blends with 10 wt % of the copolymers. In addition, except for PLA/EPE11-10, not only high temperature but also low temperature E'' peaks were very broad, and $T_{E''}$s of the latter exceeded by 20–30°C T_gs of the plasticizers. No traces of melting of EPE19 were found on the heating thermogram of PLA/EPE19-15 blend. These results, together with the fact that no heterogeneities were found by the SEM technique in annealed PLA/EPE11 and in PLA/EPE19, proved that phase separation in these materials led to the formation of plasticizers enriched phases but not to the formation of distinct inclusions of plasticizers like those detected by SEM in the PLA/P10 blends.

Tensile properties of the annealed blends depended on a plasticizer type and content. Crystallization improved drawability of the blends with 10 wt % of plasticizers, which was reflected in the lower yield stress and larger elongation at break. Annealing caused an increase in $T_{E''}$s of peaks corresponding to glass transition of the PLA rich phase, but also broadening of these peaks. The beginning of glass transition was shifted to room temperature, which increased sufficiently segmental mobility of the amorphous phase to enable plastic deformation. It can be noticed that the annealed PLA/P10 exhibited lower yield stress and larger elongation at break than annealed PLA/EPE11-10 and PLA/EPE19-10, and also T_g of the PLA rich phase of PLA/P10-10 was markedly lower than that of PLA/EPE11-10 and PLA/EPE19-10. Moreover, phase separation of the plasticizer in the form of liquid inclusions does not deteriorate the drawability, as it was demonstrated in Ref. 17.

Annealing of the blends with 15 wt % of plasticizers caused an elevation of yield stress and reduced elongation at break. In addition, the annealed PLA/P10-15 exhibited a slightly higher yield stress and shorter elongation at break than the annealed PLA/P10-10; most probably as a result of an increase in T_g of the PLA rich phase due to enhanced phase separation. Contrary to PLA/P10-15, the annealed blends with 15 wt % of copolymers, yielded at lower stresses and exhibited a marked increase in strain to fracture in comparison to the corresponding annealed blends with 10 wt % copolymers. An increase of the copolymer contents in the annealed blends was accompanied by a further decrease in $T_{E''}$ of the E'' peak of the PLA rich phase, despite the phase separation. This peak also broadened; the beginning of the glass transition was shifted far below room temperature. The enhanced mobility of the PLA rich phase undoubtedly contributed to improved drawability of these materials when compared with the corresponding blends with lower plasticizers contents.

However, the drawability of the annealed blends with 15 wt % of plasticizers was worse than that of the corresponding materials before annealing, which was reflected in the increased yield stress and reduced elongation at break. Obviously, crystallinity was a dominating factor which worsened the drawability of these materials, although to different extent, depending on a plasticizer type.

CONCLUSIONS

PEG–b-PPG–b-PEG copolymers effectively plasticized amorphous PLA. The blends of PLA with the 10 wt % of EPE11 or PPG were homogeneous, whereas PLA/EPE19-10 and the blends with 15 wt % of plasticizers exhibited signs of phase separation. Annealing caused crystallization-induced phase separation in all the blends. The structure of phase separated blends depended on the plasticizer type; in the blends with copolymers containing PEG blocks no distinct inclusions were found by SEM, unlike in the blends with PPG. Moreover, in the case of phase separated blends with copolymers, especially those annealed, E'' dependencies on temperature are suggestive of a broad spectrum of relaxation times, both in the PLA rich phase and in the copolymer rich phase. Differences between the blends with PPG and those with the copolymers undoubtedly result from the presence of PEG blocks in the copolymers molecules. In addition, PLA crystallization was more enhanced in the blends with copolymers than with PPG.

The influence of copolymers on the ductility of amorphous PLA was similar to that of PPG. The plasticizer content of 15 wt % was required to improve the drawability regardless of the plasticizer used. Annealing of the blends led to different results, depending on the plasticizer type and content. The annealed blends with 10 wt % of plasticizers exhibited improved drawability, that is, a decreased yield stress and elongation at break enlarged from 3 to 10 times, in comparison with the same materials before annealing. Contrary to this, annealing of the blends with 15 wt % of plasticizers increased the yield stresses, whereas elongations at break decreased 7–8 times for PLA with the copolymers and 16 times for PLA with PPG. Nevertheless, the plasticized systems were markedly more ductile after annealing than the annealed neat PLA, with elongation at break up to 12 times larger. It can be concluded that despite their higher molecular weight both triblock copolymers used were as useful and

effective in the plasticization of PLA as PPG. Moreover, copolymers with molecular characteristics similar to those used in the study are easily available being produced on industrial scale.

References

1. Sinclair, R. G. J Macrom Sci: Pure Appl Chem 1996, A33, 585.
2. Sodergard, A.; Stolt, M. Prog Polym Sci 2002, 27, 1123.
3. Drumright, R. E.; Gruber, P. R.; Henton, D. E. Adv Mater 2000, 12, 1841.
4. Pluta, M.; Galeski, A. J Appl Polym Sci 2002, 86, 1386.
5. Perego, G.; Cella, G. D.; Bastioli, C. J Appl Polym Sci 1996, 59, 37.
6. Bechtold, K.; Hillmyer, M. A.; Tolman, W. B. Macromolecules 2001, 34, 8641.
7. Nijenhuis, A. J.; Colstee, E.; Grijpma, D. W.; Pennings, A. J. Polymer 1996, 37, 5849.
8. Labrecque, L. V.; Kumar, R. A.; Dave, V.; Gross, R. A.; McCarthy, S. P. J Appl Polym Sci 1997, 66, 1507.
9. Ljungberg, N.; Wesslen, B. J. Appl Polym Sci 2002, 86, 1227.
10. Jacobsen, S.; Fritz, H. G. Polym Eng Sci 1999, 39, 1303.
11. Sheth, M.; Kumar, R. A.; Dave, V.; Gross, R. A.; McCarthy, S. P. J Appl Polym Sci 1997, 66, 1495.
12. Martin, O.; Averous, L. Polymer 2001, 42, 6209.
13. Baiardo, M.; Frisoni, G.; Scandola, M.; Rimelen, M.; Lips, D.; Ruffieux, K.; Wintermantel, E. J Appl Polym Sci 2003, 90, 1731.
14. Hu, Y.; Rogunova, M.; Topolkaraev, V.; Hiltner, A.; Baer, E. Polymer 2003, 44, 5701.
15. Kulinski, Z.; Piorkowska, E. Polymer 2005, 46, 10290.
16. Kulinski, Z.; Piorkowska, E.; Gadzinowska, K.; Stasiak, M. Biomacromolecules 2006, 7, 2128.
17. Piorkowska, E.; Kulinski, Z.; Galeski, A.; Masirek, R. Polymer 2006, 47, 7178.
18. Pluta, M.; Paul, M. A.; Alexandre, M.; Dubois, Ph. J Polym Sci Part B: Polym Phys 2006, 44, 312.
19. Hu, Y.; Hu, Y. S.; Topolkaraev, V.; Hiltner, A.; Baer, E. Polymer 2003, 44, 5711.
20. Drieskens, M.; Peeters, R.; Mullens, J.; Franco, D.; Lemstra, P. J.; Hristova-Bogaerds, D. G. J Polym Sci Part B: Polym Phys 2009, 47, 2247.
21. Jia, Z.; Tan, J.; Han, C.; Yang, Y; Dong, L. J Appl Polym Sci 2009, 114, 1105.
22. Ran, X.; Jia, Z.; Han, C.; Yang, Y.; Dong, L. J Appl Polym Sci 2010, 116, 2050.
23. Younes, H.; Cohn, D. Eur Polym J 1988, 24, 765.
24. Bailey, F. E. Jr.; Koleske, J. V. Poly(ethylene oxide); Academic Press: New York, 1976, p 23.
25. Sarasua, J. R.; Prud'homme, R. E.; Wisniewski, M.; Le Borgne, A.; Spassky, N. Macromolecules 1998, 31, 3895.
26. Stoclet, G.; Seguela, R.; Lefebvre, J. M.; Elkoun, S.; Vanmansart, C. Macromolecules 2010, 43, 1488.
27. Zhang, J.; Tashiro, K.; Tsuji, H.; Domb, A. J. Macromolecules 2008, 41, 1352.